

Evaluation of boron-enriched plastic scintillator for thermal neutron detection

To cite this article: V.V. Porosev and G.A. Savinov 2019 *JINST* **14** P06003

View the [article online](#) for updates and enhancements.



IOP | ebooks™

Bringing you innovative digital publishing with leading voices to create your essential collection of books in STEM research.

Start exploring the [collection](#) - download the first chapter of every title for free.

Evaluation of boron-enriched plastic scintillator for thermal neutron detection

V.V. Porosev^{a,b,1} and G.A. Savinov^a

^a*Budker Institute of Nuclear Physics,
Lavrentiev ave. 11, Novosibirsk 630090, Russia*

^b*Novosibirsk State University,
Pirogova st. 2, Novosibirsk 630090, Russia*

E-mail: porosev@inp.nsk.su

ABSTRACT: In recent years, we could observe significant progress in the design of accelerator-based neutron sources for boron neutron capture therapy (BNCT). An important component of such systems is a neutron-sensitive detector system capable of monitoring the patient dose at significantly higher particle rates than in nuclear reactor systems. Simultaneous operation of two detectors: the first, sensitive to gammas, and the second, sensitive to gammas and neutrons, enables more accurate extraction of the neutron contribution. Scintillator-based detectors with fiber-optic readout have several important advantages. They are compact and have high speed, and additionally, the readout electronics can be placed far from the neutron source. In this research, we evaluated the main parameters of two plastic scintillators that are produced in Russia and meet this goal: SC-301 and boron-enriched SC-331. The resulting light yield of SC-331 was 8600 photons/MeV, and for SC-301 it was approximately 25% higher. Therefore, these scintillators are promising candidates for future detector systems.

KEYWORDS: Detector modelling and simulations I (interaction of radiation with matter, interaction of photons with matter, interaction of hadrons with matter, etc); Neutron detectors (cold, thermal, fast neutrons); Scintillators, scintillation and light emission processes (solid, gas and liquid scintillators)

¹Corresponding author.

Contents

1	Introduction	1
2	Problem overview	1
2.1	Experimental setup	2
2.2	Single-photoelectron response of PMT	4
2.3	Light emission spectrum of scintillator	5
2.4	Reflection coefficient of photocathode	5
2.5	Light collection efficiency	6
3	Results and discussion	7
4	Conclusion	8

1 Introduction

A new generation of accelerator-based neutron sources for BNCT imposes new requirements on the diagnostic equipment monitoring the neutron contribution to the total dose of radiation. Simultaneous operation of two detectors: the first, sensitive to gammas, and the second, sensitive to gammas and neutrons, enables more accurate extraction of the neutron contribution. An example of such systems is twin tissue-equivalent proportional counters [1]. Scintillator-based detectors can achieve significantly higher performance and they are more compact as compared with gas detectors. An example is the high-performance detector of thermal neutrons based on ZnS(Ag)/LiF [2]. For medical applications, detectors based on scintillators with optical fiber readout were developed in Japan [3, 4].

A series of polystyrene-based plastic scintillators was designed in early 2000 at the Institute for High-Energy Physics (IHEP, Protvino) [5], including SC-301, without boron, and SC-331, enriched with boron, which have a fast response of ~ 2.5 ns [6]. According to their specifications, both of them use the same fluors (p-terphenyl, POPOP). In addition, the scintillator SC-331 contains 0.9% natural isotope Boron-10. Numerous parameters describing scintillators include ‘Light yield relative to anthracene’. The present research was aimed at measurement of a more robust parameter, the absolute light yield of scintillator, to predict the possible signal values in the future detector systems.

2 Problem overview

Definition of the absolute light yield of scintillator is a rather difficult task [7]. It includes measurements of many additional parameters:

- Signal value for a predefined energy deposit.
- Single photoelectron response of the photodetector.

- Quantum efficiency of the photodetector.
- Emission spectrum of the scintillator.
- Light collection efficiency.

Some parameters can be measured with good accuracy, but some, e.g. the light collection efficiency, can be estimated with much lower accuracy. In this work we studied the light output of different scintillators using a photomultiplier tube (PMT) R10233 (HAMAMATSU). Using a large PMT lets us assume that we will have 100% photoelectron collection efficiency at the center of the photocathode. In the above list, the spectral dependence of the PMT quantum efficiency $QE_{\text{PMT}}(\lambda)$ is known from the manufacturer's data [8].

2.1 Experimental setup

For the tests, we made scintillator samples with dimensions of $9 \times 9 \times 5$ mm, all the faces of which were mechanically polished. The top and side faces were coated with the EJ-510 paint (Eljen Technology).¹ During the tests, the scintillators were mounted using the optical grease BC-630 (Saint-Gobain Crystals)² on the entrance window of the photomultiplier tube. The operating voltage for the PMT (-950 V) was generated by a digital multichannel analyzer DT5780 (CAEN)³ and applied with a voltage divider E1198-26 (HAMAMATSU). The output signal from 50-Ohm load was integrated using a desktop waveform digitizer DT5720 (CAEN). A schematic view of the experimental setup and a scintillator sample are presented in figure 1.

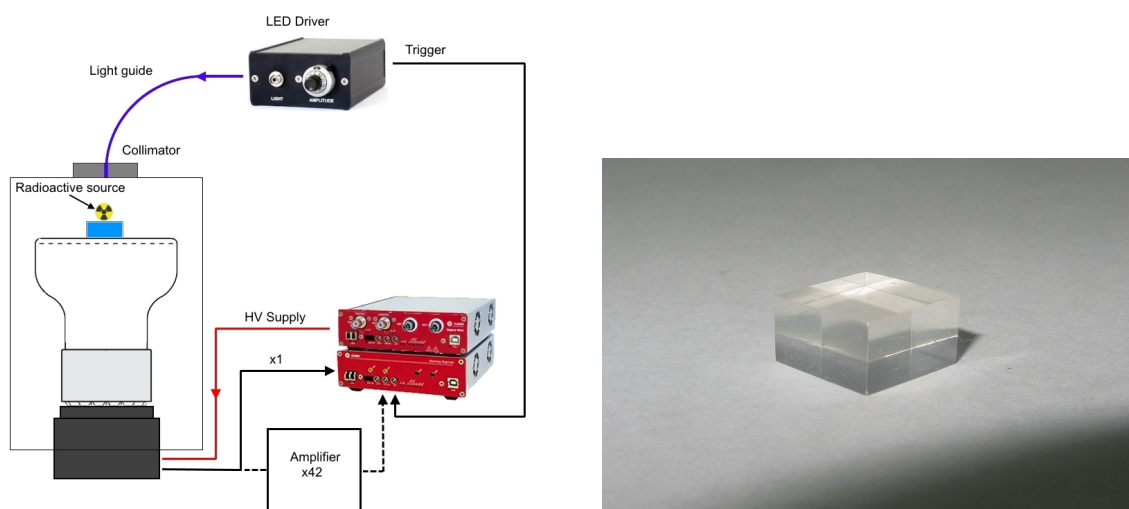


Figure 1. Schematic overview of experimental setup (left) and plastic scintillator sample (right).

To evaluate the relative light yield of two scintillators we accumulated the ‘Charge-Integration’ spectra using the isotope Am-241 as a gamma source. Figure 2 presents the spectra measured with different scintillators. The sufficiently large size of the scintillators made it possible to observe in

¹<https://eljentechnology.com>.

²<https://www.crystals.saint-gobain.com/products/assembly-materials>.

³<https://www.caen.it>.

the collected data the photopeaks from photons with an energy of 59.5 keV. The mean signal value was 229 ± 0.2 area units (A.U.) and 171 ± 0.2 A.U. for SC-301 and SC-331, respectively. It means that the relative brightness of the boron-enriched scintillator is 75% of that of the boronless one.

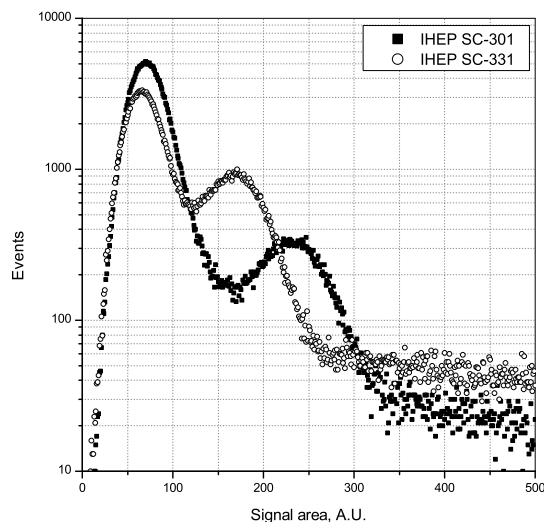


Figure 2. Energy spectrum of a Am-241 source measured with different scintillators.

To get the relative signal value with thermal neutrons, we installed the detector on the BNCT facility at BINP [9] and accumulated data during test sessions of the accelerator. At that time, the accelerator worked at energy just above the neutron production threshold. The integrated spectra for the two scintillators are presented in figure 3. To estimate the effect of induced radioactivity in the examination room, we accumulated the background signals when the accelerator was off for a compatible time. These data are shown in figure 3 too.

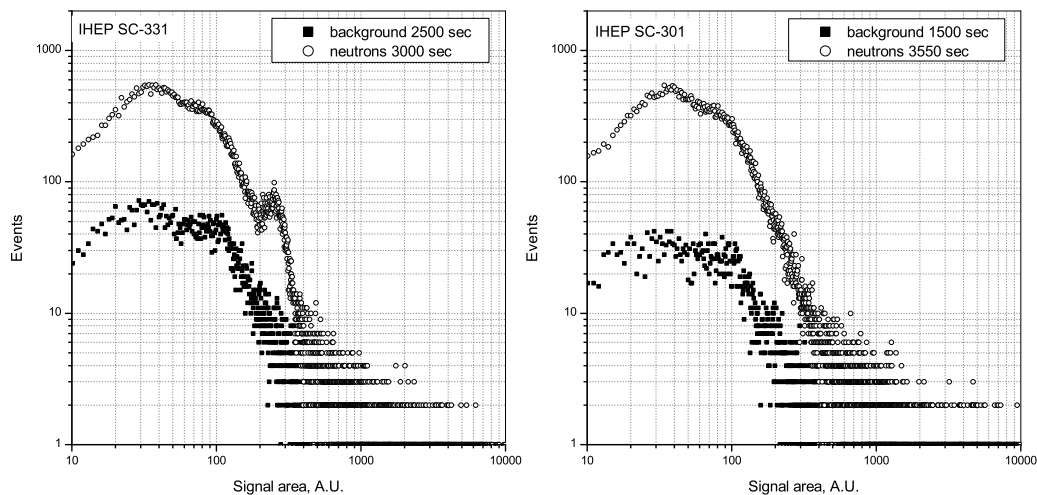


Figure 3. Energy spectra from different scintillators with (left) and without (right) boron.

In the spectrum acquired using SC-331, one can clearly see a peak related to neutron detection with a mean signal value of 259.1 ± 1.1 A.U. (FWHM of 68.2). In comparison with the Am-241 data, the mean energy deposit is equivalent to ~ 90 keV.

2.2 Single-photoelectron response of PMT

To obtain a single-photoelectron response (SPR), we exposed the PMT to light pulses generated by the ultra-fast LED Driver SP5601 (CAEN) with a wavelength of 405 nm. To clearly distinguish single-photoelectron pulses from electronics noise, we additionally amplified the signal 42-fold using a home-made OPAMP based on OPA847IDBVT (Texas Instruments).⁴ The histograms were parameterized using a combination of distributions, Gaussian for noise and Polya for SPR. The Polya distribution describes multi-step electron multiplication in the PMT taking into account the possible gain non-uniformity of the dynodes [10, 11]. We used the following parameterization in the fits [12]:

$$P(Q) = C_0 \cdot \frac{(1 + \theta)^{(1+\theta)}}{\Gamma(1 + \theta)} \left(\frac{Q}{\bar{Q}}\right)^\theta e^{-(1+\theta)\frac{Q}{\bar{Q}}}, \quad (2.1)$$

where \bar{Q} is the mean signal value and θ is a parameter of the Polya distribution. An example of accumulated histogram and the resulting SPR is shown in figure 4. Finally, we have found that in measurements without the use of an additional amplifier, the magnitude of the signal corresponding to 1 photoelectron was 2.1 ± 0.1 A.U. Table 1 summarizes the signal magnitude values for different particles.

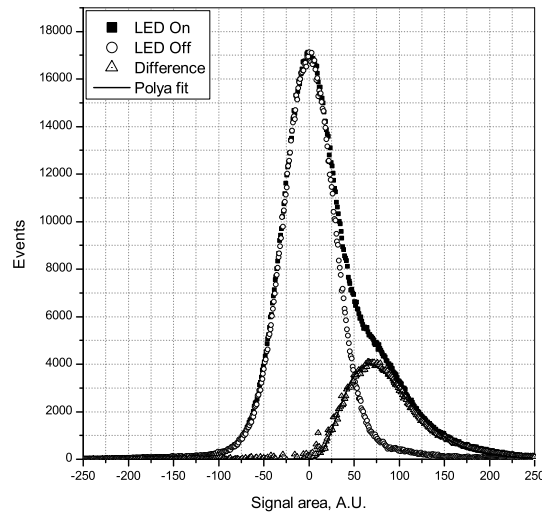


Figure 4. Pulse height spectra with LED On/Off and resulting SPR. The solid line is the Polya fit.

Table 1. Light yield of scintillators (in photoelectrons).

Scintillator	Particle/Energy	Light yield (photoelectrons)
SC-301	$\gamma/59.5$ keV	109.1 ± 4.7
SC-331	$\gamma/59.5$ keV	81.4 ± 4.5
SC-331	<i>neutron</i> /thermal	123.4 ± 5.3

⁴<http://www.ti.com>.

2.3 Light emission spectrum of scintillator

The measurements of the emission spectra were carried out on a stand based on the monochromator MDR-12U (LOMO, St.Petersburg), equipped with the photo-diode C10439-03 (HAMAMATSU). The scintillators were excited by the UV LED (UVTOP300-HL-TO39, ROITHNER LASERTECHNIK GmbH)⁵ with a wavelength of 305 nm, near the maximum of photoabsorption of the primary fluor. The emission spectrum of this kind of scintillators has the same shape as when excited by light with wavelength in the range of 260–290 nm [13]. Moreover, we can expect that the position of the maximum in the emission spectrum does not change significantly when the scintillator is excited by x-rays, because its emission is defined mainly by the wavelength-shifting fluor [14]. Figure 5 demonstrates the excited sample and its emission spectrum.

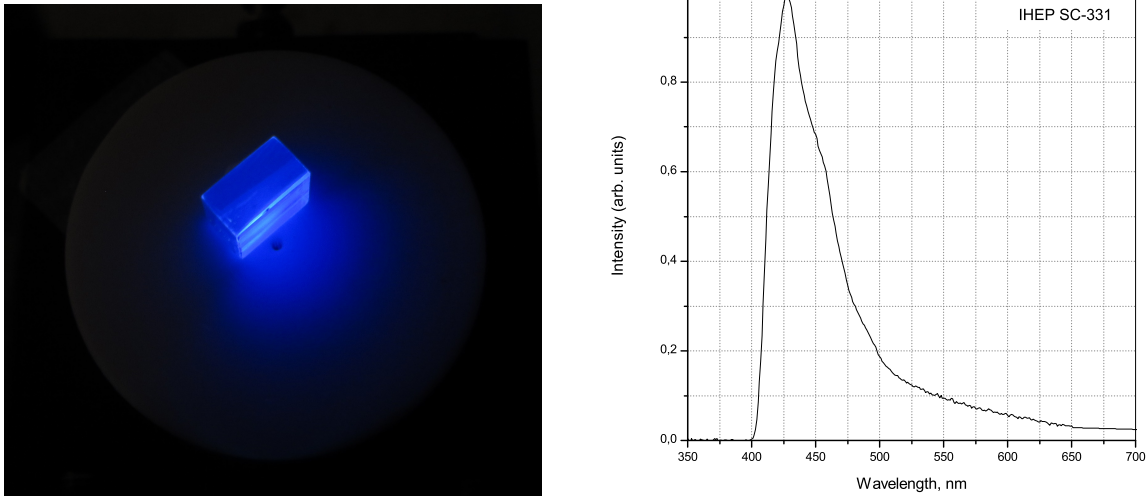


Figure 5. Light emission of sample (left) and its spectrum (right).

Since the data were measured using a monochromator with a diffraction grating, the true spectrum was restored using the dependence of the reflection coefficient $\Phi_k(\lambda)$ on the wavelength, the order of the spectrum k , and the wavelength with the highest intensity in the spectrum of the first order $\lambda_{1,0}$, known from the grid data sheet, according to the following expression [15]:

$$\Phi_k(\lambda) = \left[\frac{\sin \pi(k - \frac{\lambda_{1,0}}{\lambda})}{\pi(k - \frac{\lambda_{1,0}}{\lambda})} \right]^2. \quad (2.2)$$

2.4 Reflection coefficient of photocathode

Determination of the PMT photocathode reflection is one of the most critical steps in the measurement of the light yield of scintillators [16], since the standard scheme for measuring the quantum efficiency of a photomultiplier excludes the possibility of re-registration of optical photons reflected from the photomultiplier. The absolute value of the reflection coefficient from the photocathode of PMT R10233 was measured at near normal incidence ($\Theta = 7^\circ$) on the same stand using a halogen lamp (“LOMO PHOTONIC, St.Petersburg”),⁶ with a ‘VW’ accessory PZOM-VW (“OKB

⁵<http://www.roithner-laser.com>.

⁶<http://lomophotonica.ru>.

SPECTR”, St.Petersburg)⁷ capable to handle rather large PMTs. The term ‘VW’ is a graphical presentation of the light path through the accessory in the reference and measurement positions. This unique arrangement uses the same optical elements in both cases and allows one to measure the reflection coefficient without any additional reference standards. Figure 6 (left) presents the general view of the setup and measured reflectance spectrum (right). In the maximum of the spectral emission of the scintillators, the reflectance reaches a value of $\sim 22\%$, which correlates well with data for bialkali photocathodes [17]. The solid line shows the air-to-glass boundary contribution to the reflection, calculated in accordance with the Fresnel equations for the case of normal incidence. Thus, the true value of the reflection coefficient of photocathode $R_{\text{ph.cath.}}(\lambda)$ is the difference of these two curves.

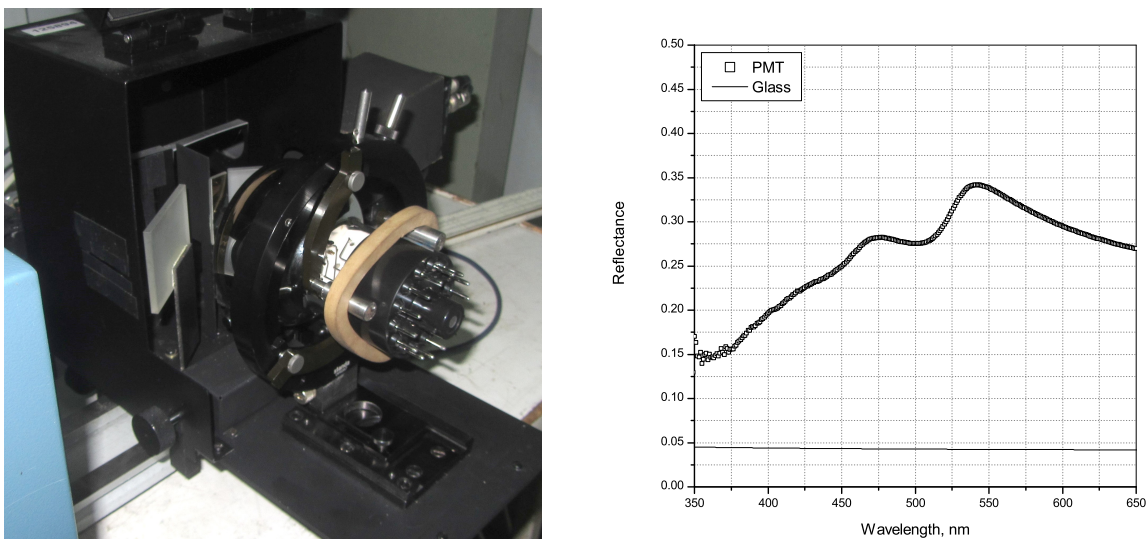


Figure 6. VW accessory with mounted PMT (left) and reflectance spectrum of R10233 (right). Total PMT reflectance (dots) and reflectance from glass envelope (solid line) are shown.

2.5 Light collection efficiency

The light collection efficiency depends on many parameters, e.g. the optical properties of scintillator, surface quality, reflection coefficient of the coating etc. Therefore, the accuracy of this parameter is limited. To estimate the light collection efficiency in the current setup we performed Monte-Carlo simulations using Geant4-10.5 [18]. The main parameters used in the simulations and their data sources are presented in table 2. The chemical composition of the optical grease BC-630 was taken the same as that of the most popular technical polymeric material, polydimethylsiloxane. The photomultiplier surface was simulated as a polished borosilicate window followed by a photocathode with the reflectivity $R_{\text{ph.cath.}}(\lambda)$ and the efficiency $QE_{\text{PMT}}(\lambda)$. To take into due account of the surface roughness, we varied the parameter SIGMA_ALPHA of GEANT4 of the painted sides in the range of $1-10^\circ$, but in reality it changes the number of detected optical photons by less than 1%. From the simulation it follows that the PMT detects 19% of the light produced in a scintillator.

⁷<http://okb-spectr.ru>.

Table 2. Main parameters used in the simulations.

Parameter	Value	Source
EJ-510 Reflection	depending on wavelength	[19]
EJ-510 Refraction index	1.61	[20]
Polystyrene refraction index	depending on wavelength	[21]
Polystyrene absorption length	depending on wavelength	[22]
Polystyrene density	1.05 g/cm ³	
BC-630 Refraction index	1.465	[23]
Borosilicate glass density	2.23 g/cm ³	
Borosilicate glass refraction index	depending on wavelength	[24]
Physics list	QGSP_BIC_AllHP + G4OpticalPhysics	

3 Results and discussion

The results of the measurements of the light output of the boron-enriched scintillator exposed to photons with an energy of 59.5 keV give us an absolute value of the scintillator light output of 7200 ± 550 photons/MeV. Nonproportionality is a well known effect, which significantly changes the light yield of scintillators, especially in detection of low energy x-ray quanta. For plastic scintillators, the light output can be about 83%, when the scintillator is excited by electrons and gammas with an energy of ~ 60 keV [25, 26]. Taking this effect into account, we can expect that the real magnitude of the light yield is ~ 8600 photons/MeV at least.

Using this value, we can simulate the detector response in particle detection. To do that in GEANT4, we should additionally determine the Birks constant of the material [27]. Determination of this value is quite a complicated procedure, so we used the value acquired from analysis of published works. For scintillators based on polystyrene, values in the range of $8 \cdot 10^{-3} - 9 \cdot 10^{-3} \text{ g MeV}^{-1} \text{ cm}^{-2}$ [28–30] are reported. Values of 0.126 mm/MeV [31] and even $1.4 \cdot 10^{-2} \text{ g MeV}^{-1} \text{ cm}^{-2}$, which provides more realistic results, are used in the simulations. The main reason is the fact that at lower nuclear recoil energies, the Birks model disagrees with experimental data [32]. In addition, in Monte-Carlo calculations, when a particle is traced by steps, it is necessary to introduce an effective Birks constant, depending on the step size [33]. Table 3 presents results of the calculations of the number of detected optical photons in the current setup with different step limits (the maximum fraction of energy loss in a step and the maximum step), parameter kB of the Birks model, and the range cut for secondary particle production, which defines if particles with a range exceeding a given value will be created and traced further or their energy will be deposited locally. For comparison, the ranges of electrons with an energy of 60 keV and α -particles with an energy of 1.8 MeV in polystyrene, calculated in accordance with continuous slowing down approximation, are 57 and 8.3 μm , respectively [34].

It is clearly seen that the results of the simulations depend strongly on GEANT4 settings. It may mean that the simulations are not correct under these conditions and the accuracy of the models used in GEANT4 for particles with high linear energy transfer is still an open issue [35].

Table 3. Calculated light yield of scintillator SC-331 (in photoelectrons) for particles in experimental setup. Data for different combination of parameters are presented. Birks constant $kB = 0.133$ mm/MeV.

Parameters	Light Yield (phe.), $\gamma/59.5$ keV	Light Yield (phe.), <i>neutron/0.1</i> eV
ProductionCut: 100 μ m Step limits: e^\pm (0.2, 0.01 mm) muons/hadrons (0.1, 0.02 mm)	76.5	106
ProductionCut: 10 μ m Step limits: e^\pm (0.2, 0.01 mm) muons/hadrons (0.1, 0.02 mm)	69.9	106
ProductionCut: 1 μ m Step limits: e^\pm (0.2, 0.01 mm) muons/hadrons (0.1, 0.02 mm)	68.3	162
ProductionCut: 1 μ m Step limits: e^\pm (1E-5, 1 μ m) muons/hadrons (1E-5, 1 μ m)	67.8	168
ProductionCut: 1 μ m Step limits: e^\pm (1E-5, 0.1 μ m) muons/hadrons (1E-5, 0.1 μ m)	63.7	170
ProductionCut: 5 μ m Step limits: e^\pm (0.1, 5 μ m) muons/hadrons (0.1, 5 μ m)	77.0	120

4 Conclusion

In this study, we measured the main characteristics of the plastic scintillators SC-301 and SC-331. Simulation based on the obtained values made it possible to estimate the expected signals in the detector, and the calculated values are in rather good agreement with the data obtained in the experiment. We think that these scintillators are good candidates for use in future detecting systems in BNCT. Nevertheless, the nonproportionality of the scintillators is still an issue to resolve in future research.

Acknowledgments

We would like to thank the BINP BNCT team for their help during the test sessions and S.K. Chernichenko (IHEP, Protvino) for the scintillator samples provided. The research is supported by a grant of the Russian Science Foundation (project №19-72-30005).

References

- [1] D. Moro et al., *BNCT dosimetry performed with a mini twin tissue-equivalent proportional counters (TEPC)*, *Appl. Radiat. Isot.* **67** (2009) 171.
- [2] V.S. Litvin et al., *Scintillation neutron detectors based on solid-state photomultipliers and lightguides*, *Crystallogr. Rep.* **61** (2016) 106.

- [3] M. Ishikawa et al., *Early clinical experience utilizing scintillator with optical fiber (SOF) detector in clinical boron neutron capture therapy: Its issues and solutions*, *Radiation Oncology* **11** (2016) 105.
- [4] M. Ishikawa et al., *Development of real-time thermal neutron monitor using boron-loaded plastic scintillator with optical fiber for boron neutron capture therapy*, *Appl. Radiat. Isot.* **61** (2004) 775.
- [5] I.G. Britvich et al., *New Polystyrene-Based Scintillators*, *Instrum. Exp. Tech.* **45** (2002) 644.
- [6] G.I. Britvich et al., *Prototype of a neutron detector based on a boron-containing plastic scintillator*, *Instrum. Exp. Tech.* **47** (2004) 571.
- [7] M. Moszynski et al., *Absolute light output of scintillators*, *IEEE Trans. Nucl. Sci.* **44** (1997) 1052.
- [8] HAMAMATSU PMT,
http://www.hamamatsu.com/resources/pdf/etd/High_energy_PMT_TPMZ0003E.pdf.
- [9] D. Kasatov et al., *The accelerator neutron source for boron neutron capture therapy*, *J. Phys. Conf. Ser.* **769** (2016) 012064.
- [10] J.R. Prescott, *A statistical model for photomultiplier single-electron statistics*, *Nucl. Instrum. Meth.* **39** (1966) 173.
- [11] S. Donati, E. Gatti and S. Svelto, *The Statistical Behavior of the Scintillation Detector: Theories and Experiments*, *Adv. Electron. Electron Phys.* **26** (1969) 251.
- [12] T. Zerguerras, B. Genolini, V. Lepeltier, J. Peyre, J. Pouthas and P. Rosier, *Single electron response and energy resolution of a MicroOMEGAs detector*, *Nucl. Instrum. Meth. A* **608** (2009) 397 [[arXiv:0901.2882](https://arxiv.org/abs/0901.2882)].
- [13] R.N. Nurmukhametov et al., *Fluorescence and absorption of a polystyrene-based scintillator exposed to UV laser radiation*, *J. Appl. Spectrosc.* **74** (2007) 824.
- [14] T.M. Demkiv et al., *Luminescent and kinetic properties of the polystyrene composites based on BaF₂ nanoparticles*, *Nucl. Instrum. Meth. A* **810** (2016) 1.
- [15] I.V. Peysahson, *Optics of spectral instruments* (in Russian), Second edition, Leningrad branch of the publishing house Mashinostroenie, Russia, (1975).
- [16] J.T.M. de Haas, P. Dorenbos and C.W.E. van Eijk, *Measuring the absolute light yield of scintillators*, *Nucl. Instrum. Meth. A* **537** (2005) 97.
- [17] D. Motta and S. Schonert, *Optical properties of Bi-alkali photocathodes*, *Nucl. Instrum. Meth. A* **539** (2005) 217 [[physics/0408075](https://arxiv.org/abs/physics/0408075)].
- [18] J. Allison et al., *Recent developments in Geant4*, *Nucl. Instrum. Meth. A* **835** (2016) 186.
- [19] Eljen Technology, <https://eljentechnology.com/products/accessories/ej-510-ej-520>.
- [20] M. Janecek and W.W. Moses, *Simulating Scintillator Light Collection Using Measured Optical Reflectance*, *IEEE Trans. Nucl. Sci.* **57** (2010) 964.
- [21] N. Sultanova, S. Kasarova and I. Nikolov, *Dispersion properties of optical polymers*, *Acta Phys. Polon.* **A 116** (2009) 585.
- [22] J. Argyriades et al., *Spectral modeling of scintillator for the NEMO-3 and SuperNEMO detectors*, *Nucl. Instrum. Meth. A* **625** (2011) 20 [[arXiv:1004.3779](https://arxiv.org/abs/1004.3779)].
- [23] BC-630, Detector Assembly Materials, https://www.crystals.saint-gobain.com/sites/imdf.crystals.com/files/documents/detector-assembly-materials_69673.pdf.
- [24] SCHOTT – BK (Borosilicate crown),
<https://refractiveindex.info/?shelf=glass&book=SCHOTT-BK&page=N-BK7>.

- [25] P. Limkitjaroenporn et al., *Nonproportionality of electron response using CCT: Plastic scintillator*, *Appl. Radiat. Isot.* **68** (2010) 1780.
- [26] A. Nassalski et al., *Non-Proportionality of Organic Scintillators and BGO*, *IEEE Trans. Nucl. Sci.* **55** (2008) 1069.
- [27] J.B. Birks, *Scintillations from Organic Crystals: Specific Fluorescence and Relative Response to Different Radiations*, *Proc. Phys. Soc. A* **64** (1951) 874.
- [28] M. Hirschberg et al., *Precise measurement of Birks kB parameter in plastic scintillators*, *IEEE NSS/MIC* **1** (1991) 183.
- [29] V.I. Tretyak, *Semi-empirical calculation of quenching factors for ions in scintillators*, *Astropart. Phys.* **33** (2010) 40 [[arXiv:0911.3041](https://arxiv.org/abs/0911.3041)].
- [30] X. Sarazin, *Recherche de la double desintegration beta sans emission de neutrino. Le detecteur BiPo, Physique Nucleaire Experimentale [nucl-ex]*, Universite Paris Sud — Paris XI, (2012), <https://tel.archives-ouvertes.fr/tel-00705459>.
- [31] N. Akchurin et al., *Lessons from Monte Carlo simulations of the performance of a dual-readout fiber calorimeter*, *Nucl. Instrum. Meth. A* **762** (2014) 100.
- [32] L. Reichhart et al., *Quenching Factor for Low Energy Nuclear Recoils in a Plastic Scintillator*, *Phys. Rev. C* **85** (2012) 065801 [[arXiv:1111.2248](https://arxiv.org/abs/1111.2248)].
- [33] K.A. Tadday, *Scintillation Light Detection and Application of Silicon Photomultipliers in Imaging Calorimetry and Positron Emission Tomography*, Dissertation, Heidelberg University, Germany, (2011), [<https://doi.org/10.11588/heidok.00012959>].
- [34] M.J. Berger et al., *Stopping-Power and Range Tables for Electrons, Protons, and Helium Ions*, NIST Standard Reference Database 124, (2017), <https://dx.doi.org/10.18434/T4NC7P>.
- [35] A. Howard and A. Ribon, *Birks Quenching*, Geant4 Technical Forum, 18 January 2019, https://indico.cern.ch/event/780834/contributions/3288995/attachments/1782107/2899684/birks_quenching_TF18Jan20191.pdf.